

Bioimaging and photodynamic activity studies of mesoporous silica nanoparticles with incorporated photosensitizers

AI-HONG WANG^a, XIAO-QIN HUANG^b, RUI PU^b, YAN-HUAI ZHOU^{b*}, HE-MING WU^{c*}

^a Nursing college of Nanjing University of Chinens Medicine, , Nanjing, P. R. China.

^b Key Laboratory of Opto-Electronic Technology, Nanjing Normal University, Nanjing, P. R. China.

^c Institute of Stomatology, Department of Oral and Maxillofacial Surgery, Nanjing Medical University, No. 136, Hanzhong Avenue, Nanjing, P.R. China.

A multifunctional system, combining two modalities of imaging and treatment, was prepared by encapsulating hypocrellin A, a photosensitive anti-cancer drug owned fluorescence, into the mesoporous silica nanoparticles. The results showed that after incorporation inside the mesoporous silica nanoparticles, the fluorescence intensity of hypocrellin A was greatly increased and the light stability was improved accordingly. Further more, comparative study of free hypocrellin A and the incorporated one indicated that both of them can be taken up by cancer cells, but the fluorescence of the incorporated one was more obvious and stable than the free one. Besides, significant damage to such impregnated tumor cells, treated with hypocrellin A incorporated mesoporous silica nanoparticles, was observed upon irradiation with light. Above results showed that such mesoporous silica nanoparticles with incorporated hypocrellin A have great application potential in the field of fluorescence imaging based diagnose and photodynamic therapy.

(Received September 3, 2014; accepted May 7, 2015)

Keywords: Antitumor agents, Silicon compounds, Photochemistry, Nanostructures, Hypocrellin A

1. Introduction

Fluorescent imaging is an important technique to elucidate signaling pathways and perform disease diagnosis in the field of biomedical research [1-4]. Recently, there is a great increasing attention to create a multifunctional system combining two modalities into a single cost-effective “see and treat” approach, which owned the bioimaging and treatment function simultaneously. However, most of fluorescents don't have the therapeutic action and most of drugs don't have the bioimaging function, too. In order to solve this problem, some drugs were conjugated with a fluorescence dye to combine two modalities of treatment and imaging [5, 6]. Based on our previous work, we found that encapsulating drugs, owned fluorescence, inside nanoparticles to improve their fluorescence intensity and stability is an alternative method to construct above multifunctional system.

Hypocrellin A (HA), a photosensitized anticancer drug, has already been widely studied in the field of photodynamic therapy (PDT), which is a noninvasive treatment modality for a range of diseases including cancers [7-11]. Mesoporous silica nanoparticles (MSN) with incorporated hypocrellin A have been prepared and intensively studied by our research group and the research results illustrated that their photodynamic activity was superior to the free hypocrellin A [12, 13]. During our studies, we found that the fluorescence intensity and the

light stability of hypocrellin A was greatly improved after been encapsulated into mesoporous silica nanoparticles by microemulsion method. This phenomenon imply that such system can be used in fluorescence imaging based diagnose.

In order to utilize this characteristic, mesoporous silica nanoparticle with incorporated hypocrellin A (MSN-HA) was prepared by emulsion method and its bioimaging and photodynamic therapy function was exploited and studied. The results showed that after been encapsulated, the fluorescence intensity of hypocrellin A was greatly increased and the light stability was improved accordingly. In vitro experiments indicated that such MSN-HA can actively uptake by cancer cell and effectively avoid fluorescence quenching during the fluorescence microscope imaging process. Moreover, the photodynamic activity of MSN-HA was satisfied.

2. Material and methods

2.1. Agents

The purity of the HA sample obtained was higher than 98% (determined by HPLC). Triethoxyvinylsilane (TEVS), 3-aminopropyl-triethoxysilane (APTES) were purchased from Sigma. Surfactant tween-80 was

purchased from Amosco. Dulbecco's minimum essential medium (DMEM) was from Gibico. All other chemicals were of analytical grade.

2.2. Preparation and characterization of mesoporous silica nanoparticle with incorporated hypocrellin A

Mesoporous silica nanoparticle with incorporated hypocrellin A was synthesized through the hydrolyzation and polymerization of 3-aminopropyltriethoxysilane (APETS) and triethoxyvinylsilane (TEVS) in the nonpolar core of tween-80/1-butanol/water micelles. Typically, 1.30 g tween-80 and 800 μL 1-butanol were dissolving in 20 mL double distilled water by vigorous magnetic stirring to get a clear micelles solution and HA in DMF (15 mM) was dissolved by magnetic stirring in the desired molar ratios until getting a clear solution. Then 200 μL TEVS was added to the above system and the resulting solution was stirred for another 2 h. After that, 10 μL APETS was added and the system stirred for about 20 h. Finally, tween-80 and 1-butanol were completely removed by dialysis against water with a cellulose membrane (12-14 k Da molecular weight cut-off). And the result concentrations of HA in MSN-HA were 4.17 μM , 12.5 μM , 25 μM , 37.5 μM , 50 μM and 62.5 μM , separately. All above experiments were carried out in dark.

Transmission electron microscopy (TEM) was used to determine the morphology and size of the aqueous dispersion of MSN-HA, using a FEI-Tevnai G220 S-TWIN electron microscopy with an acceleration voltage of 200 kV. UV-Vis absorption spectra were recorded from 350 nm to 800 nm using a VARIAN CARY 5000 spectrophotometer in a quartz cuvette with a 1cm light path. Fluorescence spectra were measured by a Perkin-Elmer LS-50B fluorometer with an excitation wavelength of 480 nm. In vitro fluorescence image was carried out in a Zeiss fluorescence microscope equipped with CCD.

2.3. Light stability analysis

The Light stability properties of free HA and MSN-HA were investigated in air-saturated aqueous solution irradiated by a high pressure mercury lamp (500 W). And absorbance spectra of them after irradiation were recorded very 1 min.

2.4. Singlet Oxygen Detection

Singlet oxygen detection measurements were carried out using the disodium salt of 9, 10- anthracendipropionic acid (ADPA) as sensor [14-16]. Typically, the aqueous

solution of ADPA (150 μL , 5.5 mmol) was mixed with different samples, including HA and MSN-HA (3 mL). These solutions were irradiated with a 500 W high-voltage mercury lamp with 470 nm cut-off filter. The absorbance intensity at 378 nm (characteristic absorption peak of ADPA) were recorded every 30 s using spectrophotometer.

2.5. Cell Cultures

Experiments were carried out with a cervical epithelium cancer cell line originally derived from Henrietta Lacks (HeLa). Cells were grown to confluence at 37 °C and in a 5% CO₂ in dulbecco's modified eagle medium (DMEM) with 10% fetal bovine serum (FBS) in a 24-cell culture plates [17, 18].

2.6. MSN-HA uptake and in vitro imaging

MSN-HA (5 μM) and free HA (5 μM) was diluted with DMEM without FBS and added to the 24-cell culture plates, seeded cells with about 60% confluence, and incubated at 37 °C with 5% CO₂ for 4 h. Then, the cells were carefully rinsed three times with phosphate-buffered saline (PBS) and then directly imaged under a fluorescence microscope.

2.7 Photo-induced cancer cell death

The HeLa cells, treated with MSN-HA and free HA for 4 h, were irradiated by light (25 J/cm²). After 24 h incubation, the cells morphology was detected by microscope. For studying cell viability, 96-well plates were inoculated with cells at 2 \times 10⁵ /mL density overnight. The medium was removed and the wells were rinsed using sterile PBS and 100 μL serum free medium with different dosages of HA or MSN-HA was replaced into each well. After incubated overnight, the cell were irradiated by light and the percentage of dead cells was evaluated using a 3-[4,5-dimethylthiazol-2-yl]-2,5-diphenyl tetrazoliumbromide (MTT) assay.

3. Results and Discussion

3.1. Microscopic characterizations

The transmission electron microscopy (TEM) image of MSN-HA showed that the average diameter of MSN-HA was 20 nm and could be dispersed in the aqueous solution (Fig. 1). Their ultrasmall size (less than 50 nm) can help them evade capture by the RES.

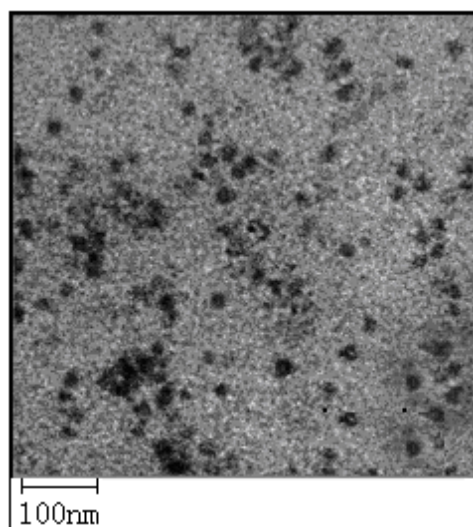


Fig. 1. The TEM image of MSN-HA.

3.2. Spectroscopic characterizations

The absorption spectra of HA and MSN-HA are similar (Fig. 2A), indicating no changes in the HA chromophore upon entrapment inside nanoparticles. However, the peaks of HA at 477 nm, 548 nm and 591 nm blue-shifted to 469 nm, 544 nm and 582 nm after incorporated into MSN. The shift of characteristic peaks maybe due to the hydrogen bonding between the -OH group of HA and the -NH₂ group of MSN.

Fig. 2B represents the fluorescence emission spectra of aqueous dispersion of free HA and MSN-HA. After encapsulation into MSN, the fluorescence intensity was greatly increased due to the protection effect of MSN, which can effectively prevent a complete loss of fluorescence of HA in aqueous environment. The property of resistance to fluorescence quenching in aqueous media of MSN-HA can be exploited as imaging reagents in biological systems.

In addition, the fluorescence intensity of MSN-HA was dependent on the concentration of incorporated HA. When the encapsulating concentration of HA was 25 μM, the fluorescence intensity reached a maximum (Fig. 3), which is much higher than the samples prepared by sol-gel method. However, when the encapsulating HA concentration continuously increased, the fluorescence intensity of MSN-HA dropped contrarily, which could be related to a fluorescence quenching effect due to the self-aggregation of HA molecules inside MSN. Therefore, the optimized concentration of HA in the MSN was 25 μM, which is much higher than the samples prepared by the sol-gel method.

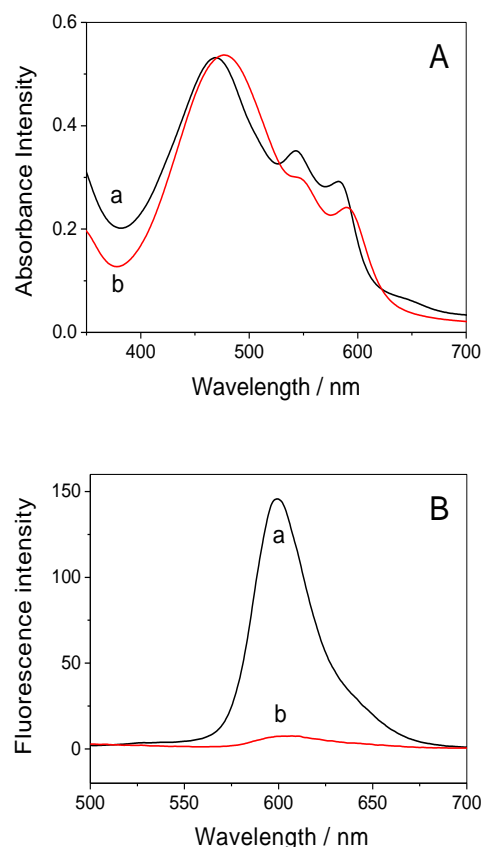


Fig. 2. The UV-Vis spectra (A) of MSN-HA (a) and free HA (b); the fluorescence spectra (B) of MSN-HA (a) and free HA (b).

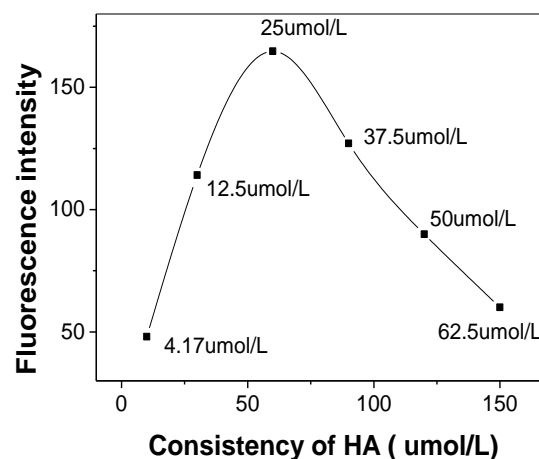


Fig. 3. Fluorescence emission spectra of MSN-HA with different concentration of HA.

To get more evidence to verify that HA had been successfully embedded into MSN and make sure that HA cannot release from MSN, fluorescence quenching experiments were conducted using triethylamine and aniline as fluorescence quencher of HA. The results in Fig. 4 indicated triethylamine can remarkably quench the fluorescence of MSN-HA; but aniline almost cannot quench the fluorescence of MSN-HA. Above results demonstrated that HA was successfully embedded into silica nanocarrier but not absorbed on the outside surface of the nanocarrier because the aniline molecule almost cannot quench the fluorescence of HA inside the nanocarrier [12]. Furthermore, based on the density functional theory, the molecular width and length of HA was bigger than aniline. So the encapsulated HA cannot be released from MSN.

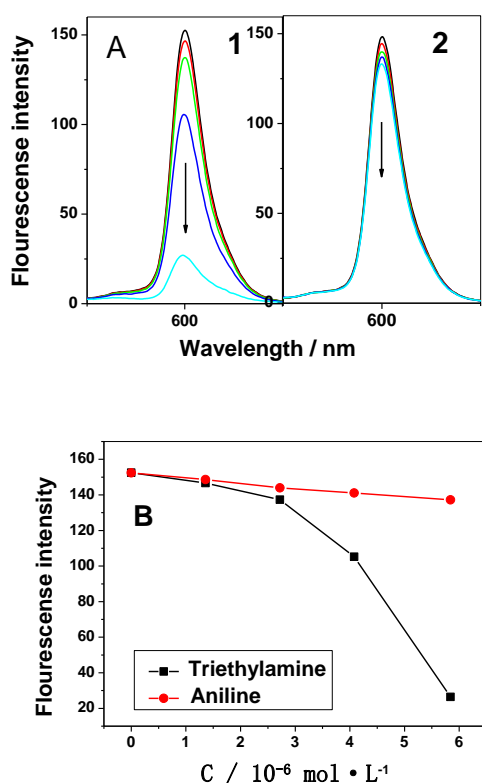


Fig. 4. Fluorescence quenching of MSN-HA by triethylamine (A1) and aniline (A2) and their quenching degree comparing (B).

3.3. Light stability

Fig. 5 insert panel showed the decrease of absorption intensity at 469 nm as a function of the irradiation time.

The result indicated that after incorporation, most HA molecules could maintain their integrity under laser irradiation as compared to the case of free HA. The protection by MSN offers better light stability of HA against bleaching [19]. The improved light stability ensure MSN-HA maintain strong fluorescence intensity during the imaging process.

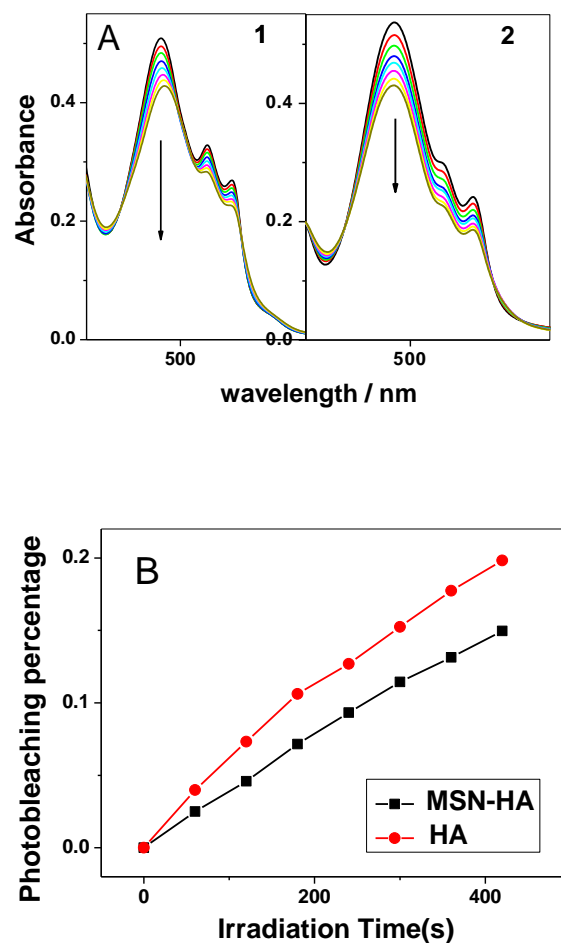


Fig. 5. MSN-HA and HA photo-bleaching process (A) and the measuring by the decrease of the absorbance at 469 nm (MSN-HA) and 477 nm (HA) as a function of irradiation time. Insert panel: photo-bleaching process of MSN-HA with the prolonged irradiation time (B).

3.4. $^1\text{O}_2$ generation

$^1\text{O}_2$ generation was detected by the method described in the experimental section, using the ADPA as detector. Fig. 6A shows the decrease in absorbance at 378 nm for MSN-HA and HAC as a function of the time of light exposure. Time-dependent bleaching of ADPA was shown

to occur severely for MSN-HA compared with that for HA, which indicates the generation of $^1\text{O}_2$ in MSN-HA is higher than that in HA.

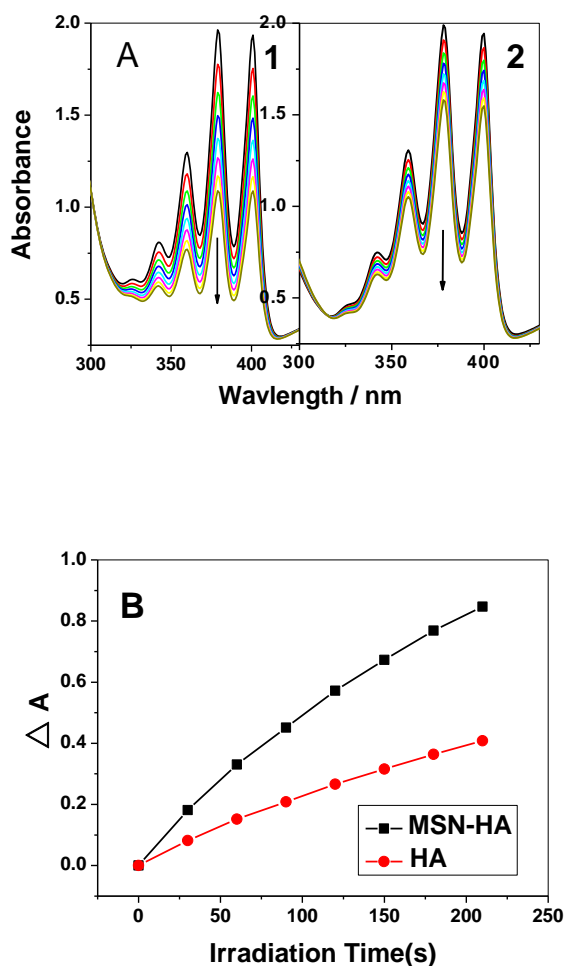


Fig. 6. (A) Absorption spectra of ADPA in MSN-HA(1) and HA(2) system were irradiated for increased time. (B) ADPA bleaching measured by the decrease of the absorbance at 378 nm as a function of irradiation time.

According to the classic equations, [20,21] the exact reaction rate constant (k) with ADPA for HA and MSN-HA were calculated by the decrease of the absorbance at 378 nm as a function of irradiation time (Fig. 7). Comparing with HA, the k value of MSN-HA was obviously increased, which indicated the $^1\text{O}_2$ generation ability of MSN-HA was higher than that of free HA.

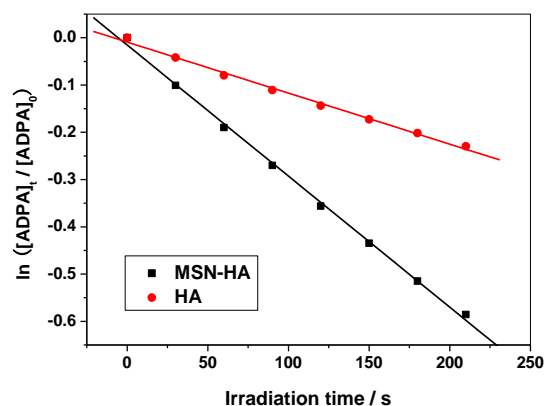


Fig. 7. ADPA bleaching of HA and MSN-HA measured by the decrease of the absorbance at 378 nm as a function of irradiation time.

3.5. Uptake and intracellular imaging of MSN-HA

Fluorescence imaging showed that both HA and MSN-HA can be taken up by cancer cells and fluoresce after excitation by light. Comparative studies showed that the fluorescence intensity of MSN-HA (Fig. 8A) was higher than free HA (Fig. 8B) in vitro and fluorescence quenching time of MSN-HA and free HA are 14 s and 10 s, separately.

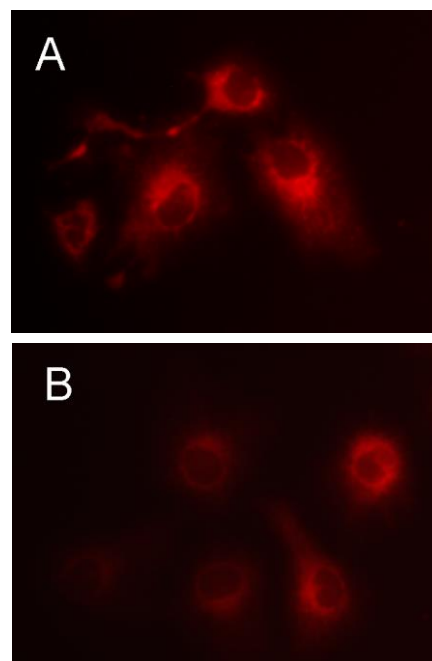


Fig. 8. Fluorescence image of HeLa cells treated with MSN-HA (A) and free HA (B).

3.6. Photo-induced anticancer activity in vitro

Further more, the photodynamic activity of MSN-HA was studied and the results showed that HeLa cells incubated in dark and treated with MSN-HA overnight did not cause any significant change in cell morphology (Fig. 9A). On the contrary, drastic changes in the morphology of HeLa cells, which were treated overnight with MSN-HA, have been observed after irradiation under the same conditions (Fig. 9B). The cells shrank and appeared many membrane blebbings.

In addition, HeLa cells were exposed to light following treatment with free HA or MSN-HA. As can be seen from Fig. 10, MSN-HA enhanced the tumor cell kill ability comparing with free HA by the MTT assay. Above results showed that MSN-HA combined two modalities of bioimaging and photodynamic therapy.

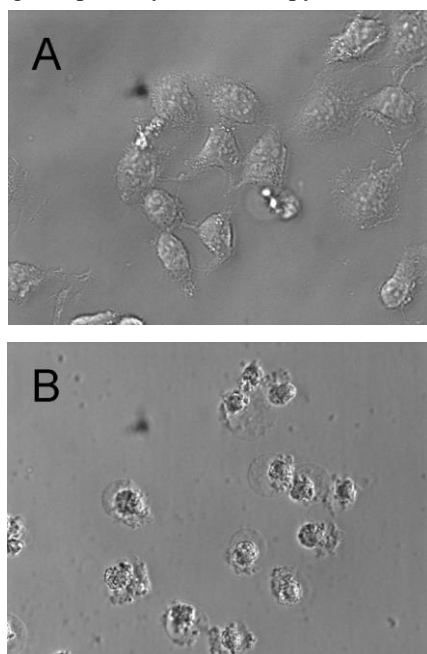


Fig. 9. Microscope morphology of HeLa cells before (A) and after (B) photodamage by light.

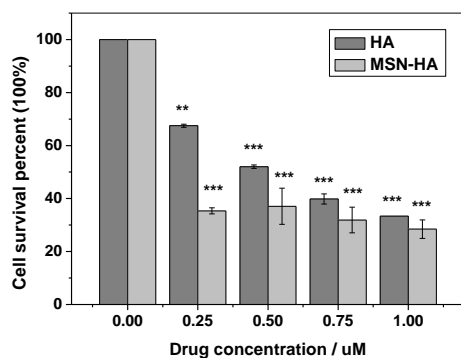


Fig. 10. Comparative in vitro drug dose affect photosensitizing efficacy of MSN-HA and HA in HeLa cells. (** $p < 0.01$ vs. Control; *** $p < 0.001$ vs. Control; Control: Cells were exposed to light without drug).

4. Conclusions

In conclusion, mesoporous silica nanoparticle containing encapsulated HA were prepared and tested for their possible applications in photodynamic therapy and biodiagnose in cancer cells. It was found that MSN-HA can enhance photodamaging ability towards cancer cells comparing with free HA. Therefore, it is reasonable to expect MSN-HA would find important uses in diagnose and PDT.

Acknowledgements

We are grateful to the key laboratory of photochemical conversion and optoelectronic materials, TIPC, CAS. The Natural Science Foundation of Jiangsu Higher Education Institutions of China (No. 11KJA510003, 11KJB360006 and 2011JSJG232); Ministry of Education Fund (10YJCZH017), Jiangsu province six talents peak project (2009-B1-037).

References

- [1] D. Mangindaan, I. Yared, H. Kurniawan, J. R. Sheu, M. J. Wang, *J. Biomed. Mater. Res. A* **100**, 3177 (2012).
- [2] I. G. Newton, W. C. Plaisted, S. Messina-Graham, A. E. A. Schairer, A. Y. Shih, E. Y. Snyder, C. H. M. Jamieson, R. F. Mattrey, *Contrast Media Molecul. Imaging* **7**, 525 (2012).
- [3] A. Pardo, M. Stocker, F. Kampmeier, G. Melmer, R. Fischer, T. Thepen, S. Barth, *Cancer Immunol. Immun.* **61**, 1617 (2012).
- [4] J. C. Tseng, Y. C. Wang, P. Banerjee, A. L. Kung, *Molecul. Imaging Biol.* **14**, 553 (2012).
- [5] S. S. Kelkar, T. M. Reineke, *Bioconjugate Chem.* **22**, 1879 (2011).
- [6] H. Skaat, S. Margel, *Biochem. Biophys. Res. Commun.* **386**, 645 (2009).
- [7] A. Babu, K. Jeyasubramanian, P. Gunasekaran, R. Murugesan, *J. Biomed. Nanotech.* **8**, 43 (2012).
- [8] L. Gao, J. B. Fei, J. Zhao, H. Li, Y. Cui, J. B. Li, *ACS Nano* **6**, 8030 (2012).
- [9] Z. Z. Ou, H. Jin, Y. Y. Gao, S. Y. Li, H. X. Li, Y. Li, X. S. Wang, G. Q. Yang, *J. Phys. Chem. B* **116**, 2048 (2012).
- [10] L. Zhou, W. Wang, Y. Y. Feng, S. H. Wei, J. H. Zhou, B. Y. Yu, J. Shen, *Bioorg. Med. Chem. Lett.* **20**, 6172 (2010).
- [11] L. Zhou, W. Wang, J. Tang, J. H. Zhou, H. J. Jiang, J. Shen, *Chem. Eur. J.* **17**, 12084 (2011).

- [12] L. Zhou, J. H. Liu, F. Ma, S. H. Wei, Y. Y. Feng, J. H. Zhou, B. Y. Yu, J. Shen, *Biomed. Microdev.* **12**, 655 (2010).
- [13] L. Zhou, J. H. Liu, J. Zhang, S. H. Wei, Y. Y. Feng, J. H. Zhou, B. Y. Yu, J. Shen, *Int. J. Pharmaceut.* **386**, 131 (2010).
- [14] K. Baba, H. E. Pudavar, I. Roy, T. Y. Ohulchanskyy, Y. H. Chen, R. K. Pandey, P. N. Prasad, *Mol. Pharmaceut.* **4**, 289 (2007).
- [15] T. Y. Hulchanskyy, I. Roy, L. N. Goswami, Y. Chen, E. J. Bergey, R. K. Pandey, A. R. Oseroff, P. N. Prasad, *Nano Letters* **7**, 2835 (2007).
- [16] S. Kim, T. Y. Ohulchanskyy, H. E. Pudavar, R. K. Pandey, P. N. Prasad, *J. Am. Chem. Soc.* **129**, 2669 (2007).
- [17] R. P. Rajesh, M. S. Ramasamy, A. Murugan, *Med. Chem.* **6**, 396 (2010).
- [18] K. Takara, T. Sakaeda, T. Yagami, H. Kobayashi, N. Ohmoto, M. Horinouchi, K. Nishiguchi, K. Okumura, *Biol. Pharm. Bull.* **25**, 771 (2002).
- [19] H. L. Tu, Y. S. Lin, H. Y. Lin, Y. Hung, L. W. Lo, Y. F. Chen, C. Y. Mou, *Adv. Mater.* **21**, 172 (2009).
- [20] L. Zhou, L. Zhou, X. F. Ge, J. H. Zhou, S. H. Wei, J. Shen, *Chem. Commun.* **51**, 421 (2015).
- [21] L. Zhou, X. F. Ge, J. H. Zhou, S. H. Wei, J. Shen, *RSC Advances.* **5**, 2794 (2015).

*Corresponding author: zhouyanhuainjnu@163.com;
whmz2002@yahoo.cn